AAC Journals.ASM.org

An NF-κB-Based High-Throughput Screen Identifies Piericidins as Inhibitors of the *Yersinia pseudotuberculosis* Type III Secretion System

Miles C. Duncan,[a] Weng Ruh Wong,[b] Allison J. Dupzyk,[a] Walter M. Bray,[b] Roger G. Linington,[b] Victoria Auerbuch[a]

Department of Microbiology and Environmental Toxicology, University of California Santa Cruz, Santa Cruz, California, USA[a]; Department of Chemistry and Biochemistry, University of California Santa Cruz, Santa Cruz, California, USA[b]

The type III secretion system (T3SS) is a bacterial appendage used by dozens of Gram-negative pathogens to subvert host defenses and cause disease, making it an ideal target for pathogen-specific antimicrobials. Here, we report the discovery and initial characterization of two related natural products with T3SS-inhibitory activity that were derived from a marine actinobacterium. Bacterial extracts containing piericidin A1 and the piericidin derivative Mer-A 2026B inhibited *Yersinia pseudotuberculosis* from triggering T3SS-dependent activation of the host transcription factor NF-κB in HEK293T cells but were not toxic to mammalian cells. As the *Yersinia* T3SS must be functional in order to trigger NF-κB activation, these data indicate that piericidin A1 and Mer-A 2026B block T3SS function. Consistent with this, purified piericidin A1 and Mer-A 2026B dose-dependently inhibited translocation of the *Y. pseudotuberculosis* T3SS effector protein YopM inside CHO cells. In contrast, neither compound perturbed bacterial growth *in vitro*, indicating that piericidin A1 and Mer-A 2026B do not function as general antibiotics in *Yersinia*. In addition, when *Yersinia* was incubated under T3SS-inducing culture conditions in the absence of host cells, Mer-A 2026B and piericidin A1 inhibited secretion of T3SS cargo as effectively as or better than several previously described T3SS inhibitors, such as MBX-1641 and aurodox. This suggests that Mer-A 2026B and piericidin A1 do not block type III secretion by blocking the bacterium-host cell interaction, but rather inhibit an earlier stage, such as T3SS needle assembly. In summary, the marine-derived natural products Mer-A 2026B and piericidin A1 possess previously uncharacterized activity against the bacterial T3SS.

Over 2 dozen Gram-negative pathogens use type III secretion systems (T3SS) to cause disease, including the causative agents of plague, pneumonia, and typhoid fever (1). These pathogens collectively cause over 200 million cases of human illness and more than half a million deaths worldwide each year (www.who.int) (2). The issue of antibiotic resistance is most pressing for Gram-negative bacteria, for which only one new class of antibiotics has been approved in the last 15 years (3, 4). While T3SS-expressing bacteria have historically been susceptible to a number of antibiotics, many antibiotic-resistant strains have recently been isolated (www.CDC.gov). As T3SS are typically required to cause disease (1), the virulence factor represents a promising target for new antimicrobial compounds.

The T3SS is composed of a basal structure spanning the inner and outer bacterial membranes and a needle that extends from the bacterial surface (5). This structure acts as a molecular syringe that injects bacterial effector proteins directly inside target host cells. While the structure of the T3SS is relatively conserved among T3SS-expressing bacteria, the suite of T3SS effector proteins expressed by each group of pathogens is completely distinct (1). The *Yersinia pseudotuberculosis* T3SS has been extensively studied and is often used as a model for T3SS-expressing pathogens (6). In *Yersinia*, the T3SS translocon proteins LcrV, YopB, and YopD form a pore in the mammalian plasma membrane upon host cell contact, enabling translocation of effector proteins inside the host cell cytosol (7). The *Y. pseudotuberculosis* effector proteins YopH, YopO, YopT, and YopE block phagocytosis and the formation of reactive oxygen species, while YopJ, YopM, and YopK dampen innate immune signaling (8, 9).

Over the past decade, a number of research groups have discovered small-molecule T3SS inhibitors by high-throughput screening (HTS) (6). These inhibitors are diverse in chemical structure, and their mechanisms of action are almost universally unknown. As virulence blockers are attractive alternatives to traditional antibiotics (10–12), discovering and better understanding new T3SS inhibitors is an important goal for anti-infectives research. In this study, we describe a unique HTS of marine-derived natural products for T3SS inhibitors that takes advantage of the ability of the *Y. pseudotuberculosis* T3SS to trigger NF-κB activation in HEK293T cells, an activity that is dependent on YopB (13). If the T3SS is rendered nonfunctional through either genetic or chemical means, host cell NF-κB activity remains at a basal level during infection. The two related small molecules discovered through this novel HTS block translocation of *Y. pseudotuberculosis* T3SS effector proteins into eukaryotic cells but do not act as general *Yersinia* antibiotics or mammalian-cell cytotoxins.

MATERIALS AND METHODS

Bacterial growth conditions. The bacterial strains used in this paper are listed in Table 1. *Y. pseudotuberculosis* was grown in 2× yeast extract-tryptone (YT) medium at 26°C with shaking overnight. The cultures were back diluted into low-calcium medium (2× YT plus 20 mM sodium oxalate and 20 mM $MgCl_2$) to an optical density at 600 nm (OD_{600}) of 0.2

Received 16 September 2013 Returned for modification 8 October 2013
Accepted 26 November 2013
Published ahead of print 2 December 2013
Address correspondence to Victoria Auerbuch, vastone@ucsc.edu.
Supplemental material for this article may be found at http://dx.doi.org/10.1128/AAC.02025-13.

doi:10.1128/AAC.02025-13

TABLE 1 *Y. pseudotuberculosis* strains used in the study

Strain	Description	References
Wild type	*Y. pseudotuberculosis* IP2666 (no YopT expression)	37
Δ*yop6*	IP2666 Δ*yopHEMOJ*	13
Δ*yop6*/Δ*yopB*	IP2666 Δ*yopHEMOJB*	13
Δ*yop6* + pYopM-Bla	IP2666 Δ*yopHEMOJ* pYopM-Bla	This work
Δ*yop6*/Δ*yopB* + pYopM-Bla	IP2666 Δ*yopHEMOJB* pYopM-Bla	This work
Δ*yscNU*	Deletion of *yscNU* operon	38

and grown for 1.5 h at 26°C with shaking, followed by 1.5 h at 37°C to induce Yop synthesis, as previously described (13).

Cell lines. HEK293T cells were maintained in Dulbecco's modified Eagle's medium (DMEM) supplemented with 10% fetal bovine serum (FBS) and 2 mM L-glutamine at 37°C in 5% CO_2. CHO-K1 cells were maintained in Ham's F-12 nutrient mixture with Kaighn's modification (F-12K) with 10% FBS and 2 mM L-glutamine at 37°C in 5% CO_2.

Natural-product library and bioassay-guided fractionation. A screening campaign for T3SS inhibitors was carried out using a marine-natural-products library. This library was generated from environmental-sediment-derived marine microorganisms specifically from the class *Actinomycetales*, known for their prolific production of pharmacologically interesting secondary metabolites. Sediment samples were collected into sterile 15-ml Falcon tubes by scuba diving, mostly from the West Coast of the United States. The supernatant was removed, and sediment samples were plated onto *Actinobacterium*-specific isolation medium with added antifungal and Gram-negative antibacterial agents by radial stamping with sterile cotton swabs. Morphologically distinct colonies were picked and replated on Difco marine broth agar plates repeatedly until pure isolates were obtained. Isolated actinobacterial colonies were subjected to liquid medium culturing using our standard fermentation conditions (see below) and cryopreserved as glycerol stock solutions at −80°C.

Frozen stocks of environmental isolates were streaked onto fresh marine broth plates (Difco, USA) and incubated at 25°C until discrete colonies became visible. Selected colonies were inoculated into 7 ml of modified saline SYP (mSYP) medium (10 g starch, 4 g peptone, 2 g yeast extract, and 31.2 g Instant Ocean in 1 liter of distilled water), and the cultures were stepped up in stages by first inoculating 2.5 ml of 3-day-old 7-ml cell cultures into 60 ml of mSYP (medium scale), followed by inoculation of 40 ml of these 2-day-old medium-scale cell cultures into 1 liter of the same broth (large scale). All cultures were incubated at 26°C and shaken at 200 rpm.

Large-scale cultures were fermented for 7 days prior to chemical extraction. Twenty grams of prewashed Amberlite XAD-16 resin (CH_2Cl_2, methanol [MeOH], and water) was added to each large-scale culture and shaken for 2 h (200 rpm), and the resulting slurry was filtered under vacuum through a glass microfiber filter (Whatman). The cells, resins, and filter paper were extracted with 1:1 CH_2Cl_2-MeOH (250 ml), and the suspension was shaken at 200 rpm for 1 h. Organic extracts were filtered and concentrated to dryness *in vacuo*. The dried crude extracts were prefractionated by solid-phase extraction chromatography (5-g C_{18} cartridge; Supelco, USA) using a stepwise MeOH-H_2O gradient: 40 ml of 10%, 20% (fraction A), 40% (fraction B), 60% (fraction C), 80% (fraction D), and 100% (fraction E) MeOH and then 100% ethyl acetate (EtOAc) (fraction F). Fractions A to F were concentrated to dryness *in vacuo* and then resuspended in dimethyl sulfoxide (DMSO) (1 ml), and aliquots of these DMSO stock solutions were reformatted into 384-well plates prior to screening.

From the primary screening of crude prefractions, active hits were selected for peak library screening to identify the active constituent(s) within a particular crude prefraction. A 45-μl aliquot of prefraction DMSO stock was lyophilized and fractionated by C_{18} reversed-phase high-performance liquid chromatography (RP-HPLC) (Phenomenex Synergi Fusion-RP; 10- by 250-mm column; 2-ml min^{-1} flow rate) using an MeOH-H_2O (0.02% formic acid) solvent system. Each prefraction was run on a gradient specifically tailored to produce the most highly resolved chromatography. The eluent was collected into deep-well 96-well plates using an automated time-based fraction collection method consisting of 1-min time slices and subsequently concentrated to dryness *in vacuo*. The dried plates were resolubilized (10 μl DMSO per well), sonicated to ensure homogeneity, reformatted into 384-well format, and subjected to secondary screening.

High-throughput screen. On day 1, 3.75×10^6 HEK293T cells were plated onto three 100- by 20-mm tissue culture dishes (BD Falcon) and incubated at 37°C and 5% CO_2. On day 2, the HEK293T cells were transfected with an NF-κB luciferase reporter plasmid (Stratagene) using Lipofectamine 2000 (Invitrogen) according to the manufacturer's instructions. This plasmid contains an NF-κB binding site (five repeats of GGA AAGTCCCCAGC) upstream of the luciferase gene. On day 3, the transfected cells were pooled, and 5×10^4 cells were transferred into each well of a 384-well plate. Each plate was centrifuged for 5 min at 290 × *g*. *Y. pseudotuberculosis* overnight cultures were back diluted into 2× YT medium to an OD_{600} of 0.2 and grown in a shaking incubator at 26°C for 1.5 h. The cultures were then pelleted by centrifugation and resuspended in half the original volume of low-calcium 2× YT medium. The bacteria were transferred to a 384-well plate containing low-calcium medium plus prefractions from the natural-product library or plain DMSO and incubated for 1.5 h at 37°C. Immediately prior to infection, prefractions or DMSO vehicle control was added to the 384-well plate containing HEK293T cells by a pinning robot. A Janus MDT pinning robot (PerkinElmer) was next used to transfer *Y. pseudotuberculosis* from the bacterial 384-well plate to the HEK293T plate at a multiplicity of infection (MOI) of 7. After 4 h at 37°C and 5% CO_2, the medium was aspirated before adding a 1:1 Neolite–phosphate-buffered saline (PBS) solution. Plates were covered in foil and incubated for 5 min, and bioluminescence was measured using an EnVision plate reader (PerkinElmer).

We used *Y. pseudotuberculosis* lacking the six known T3SS effector proteins, YopHEMOJT (Δ*yop6*), for this screen because YopHEMOJT are not required for T3SS-dependent NF-κB induction, and instead, several Yop proteins modulate NF-κB activation (8). A *Y. pseudotuberculosis* mutant lacking the T3SS translocon component YopB (Δ*yop6* Δ*yopB*) was used as a T3SS-negative control. *Y. pseudotuberculosis* Δ*yop6* in the absence of natural products triggered, on average, 12-fold-greater luminescence than the *Y. pseudotuberculosis* Δ*yop6* Δ*yopB* mutant (data not shown).

Purified T3SS inhibitors. Aurodox was purchased from Enzo Life Sciences, MBX1641 from ChemBridge, C22 from TimTec, and C15 and C24 from Princeton Biomolecular Research.

Piericidin A1 and its analog Mer-A 2026B were isolated from an *Actinomycetes* strain, RL09-253-HVS-A, isolated from a marine sediment sample collected at Point Estero, CA, at a depth of 50 feet by scuba diving. This *Actinomycetes* strain was identified as a *Streptomyces* sp. based on the typical morphology of streptomycetes, which form dry powdery spores on agar plates, and by sequencing the 16S rRNA gene (data not shown). From a large-scale culture (4 liters) of the strain producing extract 1772, 0.33 g of prefraction D was obtained (using the prefractionation method described above). The active constituents were purified using C_{18} RP-HPLC (with a gradient of 58% to 88% MeOH–0.02% formic acid-H_2O; 2 ml/min [Synergi 10μ Fusion-RP column; Phenomenex, USA]) (t_R [retention time] = 12.5 min for Mer-A 2026B and 30.5 min for piericidin A1) to give 1.6 mg of Mer-A 2026B and 2.7 mg of piericidin A1. Electrospray ionization-time of flight high-resolution mass spectrometry (ESI-TOF HRMS) analysis predicted the molecular formulae $C_{24}H_{35}NO_3$ and $C_{25}H_{37}NO_4$ for Mer-A 2026B and piericidin A1, respectively. One-dimensional ^1H nuclear magnetic resonance (NMR) spectra (see Fig. S2 and S3 in the supplemental material) were obtained using a Varian Unity Inova spec-

trometer at 600 MHz equipped with a 5-mm HCN triple-resonance cryoprobe. The spectra were referenced to residual solvent signals (δ_H [proton chemical shift] of 7.24 for d-$CDCl_3$ [deuterated chloroform]).

Mammalian cytotoxicity. HeLa cell staining was performed as previously described (14). Briefly, HeLa cells were incubated with microbial extracts for 19 h and stained with Hoechst stain to visualize individual nuclei. The 10% of natural-product fractions that most reduced HeLa nuclear counts were classified as cytotoxic to mammalian cells and excluded from follow-up. This top 10% of nucleus reduction correlated strongly with the effects of previously characterized cytotoxic compounds within the training set used by Schulze et al. (14). For unpurified natural-product fractions (including 1772D), the mammalian cytotoxicity data were generated by Schulze et al. (14). The cytotoxicity data for purified piericidin A1 and Mer-A 2026B at ≤250 μM were obtained specifically for this study.

Growth curves. Overnight cultures of wild-type (WT) *Y. pseudotuberculosis* IP2666 were back diluted to an OD_{600} of 0.2, and 100 μl was added to each well of a 96-well plate. A total of 0.3 μl of DMSO or purified natural products was added to each well. Bacteria were grown at 23°C in 2× YT medium or at 37°C in low-calcium medium (T3SS-inducing conditions), and the OD_{600} of the culture was measured every 15 min for 5 or 6 h using a VersaMax Tunable Microplate Reader (Molecular Devices). The 96-well plates were continuously shaken throughout the experiment. Additional growth curves were carried out by taking samples of bacterial cultures at 0, 3, 6, and 24 h of growth; serially diluting them; and plating them for CFU (see Fig. S5 in the supplemental material). Starting inocula of 4×10^3 or 1×10^6 CFU/ml were used. The 26°C growth curves were carried out in 500 μl of 2× YT medium with continuous shaking, while the 37°C growth curves were performed in high-calcium medium (2× YT plus 5 mM $CaCl_2$) to prevent induction of the T3SS and associated growth restriction. All growth curves used DMSO at 0.3%, piericidins at ≤143 μM, or kanamycin at 50 μg/ml.

YopM translocation assay. A total of 6×10^3 CHO-K1 cells were plated in each well of a 384-well plate in 70 μl of F-12K medium plus 10% FBS and incubated overnight. The following day, *Y. pseudotuberculosis* YopM–β-lactamase (YopM-Bla) reporter strain overnight cultures were back diluted into low-calcium 2× YT medium to an OD_{600} of 0.2 and grown in a shaking incubator at 26°C for 1.5 h. The cultures were then transferred to a 384-well plate containing low-calcium medium and purified compounds or DMSO and incubated for 1.5 h at 37°C. Immediately prior to infection, the purified compounds or DMSO was added to the 384-well plate containing CHO-K1 cells by a pinning robot (Janus MDT; PerkinElmer). The pinning robot was next used to transfer *Y. pseudotuberculosis* from the bacterial 384-well plate to the CHO-K1 plate at an MOI of 6. Five minutes after this transfer, the plate was centrifuged at 290 × *g* for 5 min to initiate bacterium-host cell contact and incubated for 1 h at 37°C and 5% CO_2. Thirty minutes prior to the end of the infection, CCF2-AM (Invitrogen) was added to each well, and the plate was covered in foil and incubated at room temperature. At the end of the infection, the medium was aspirated, and 4% paraformaldehyde was added to each well for 20 min to fix the cells. The paraformaldehyde was then aspirated, and the DNA dye DRAQ5 (Cell Signaling Technology) in PBS was added to each well. The monolayers were incubated at room temperature for 10 min, washed once with PBS, and visualized using an ImageXpress^{MICRO} automated microscope and MetaXpress analysis software (Molecular Devices). The number of YopM-Bla-positive cells was calculated by dividing the number of blue (CCF2-cleaved) cells by the number of green (total $CCF2^+$) cells. Data from three separate wells were averaged for each experiment.

Type III secretion assay. Visualization of T3SS cargo secreted in broth culture was performed as previously described (13). *Y. pseudotuberculosis* low-calcium medium cultures were grown for 1.5 h at 26°C. Purified compounds or DMSO was added, and the cultures were switched to 37°C for another 2 h. The cultures were spun down at 13,200 rpm for 10 min at room temperature, and the supernatants were transferred to a new Eppendorf tube. Ten percent (final concentration) trichloroacetic acid was added, and the mixture was vortexed vigorously. Samples were incubated on ice for 20 min and then spun down at 13,200 rpm for 15 min at 4°C. The pellet was resuspended in final sample buffer (FSB) plus 20% dithiothreitol (DTT). Samples were boiled for 5 min prior to running on a 12.5% SDS-PAGE gel. Sample loading was normalized for the bacterial density (OD_{600}) of each sample. Densitometric quantification of the bands was done using Image Lab software (Bio-Rad), setting the first DMSO-treated WT *Y. pseudotuberculosis* YopE band to 1.00.

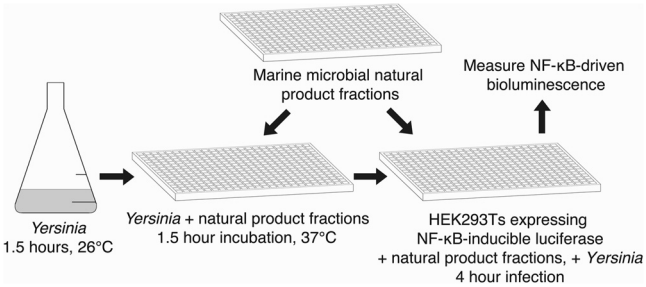

FIG 1 NF-κB-based HTS to identify small-molecule inhibitors of the *Yersinia* T3SS. *Y. pseudotuberculosis* Δ*yop6* was added to a 384-well plate containing natural-product fractions or DMSO and incubated for 1.5 h in low-calcium medium at 37°C to induce formation of the T3SS. The same natural products were robotically added to a 384-well plate containing HEK293T cells expressing an NF-κB-inducible luciferase reporter gene. The induced *Y. pseudotuberculosis* cultures were used to infect the HEK293T reporter cells at an MOI of 7. Four hours later, NF-κB-driven bioluminescence was measured and served as a readout of T3SS function in the presence of natural products.

RESULTS

Screen to identify T3SS inhibitors. To carry out our HTS (Fig. 1), we transiently transfected HEK293T cells with a plasmid carrying an NF-κB-inducible luciferase reporter gene and infected the cells with *Y. pseudotuberculosis* carrying a functional T3SS in the presence of marine-derived natural products or DMSO vehicle control. The bioluminescence intensity produced by the cultures was used as a readout of T3SS activity. The in-house natural-products library used consisted of over 5,000 partially purified "prefractions" containing 2 to 20 actinobacterium-derived small molecules per prefraction (14, 15). This library has been shown to contain compounds with specific antimicrobial activities (15) but has not previously been screened for T3SS inhibitors.

We performed the screen described above on 2,560 prefractions in duplicate. We identified 355 prefractions that reduced NF-κB-driven luminescence by 2 standard deviations below the mean of the DMSO-treated control (see Dataset S1 in the supplemental material). This pool of prefractions may contain T3SS inhibitors but may also contain compounds toxic to eukaryotic cells, killing the HEK293T cells before robust NF-κB activation can be induced. For instance, the known cytotoxins staurosporine and gliotoxin lowered NF-κB-driven luminescence to 7- and 11-fold less than that induced by the Δ*yop6* Δ*yopB* T3SS-deficient strain, respectively (Fig. 2A). To exclude prefractions containing potently cytotoxic compounds, we eliminated 217 prefractions that reduced T3SS-driven luminescence to at least 1 standard deviation below the average luminescence produced by the Δ*yop6* Δ*yopB*-infected cells (see Dataset S1 in the supplemental material). A total of 92% of these eliminated prefractions also showed HeLa cell cytotoxicity in work by Schulze et al. (14), validating this approach.

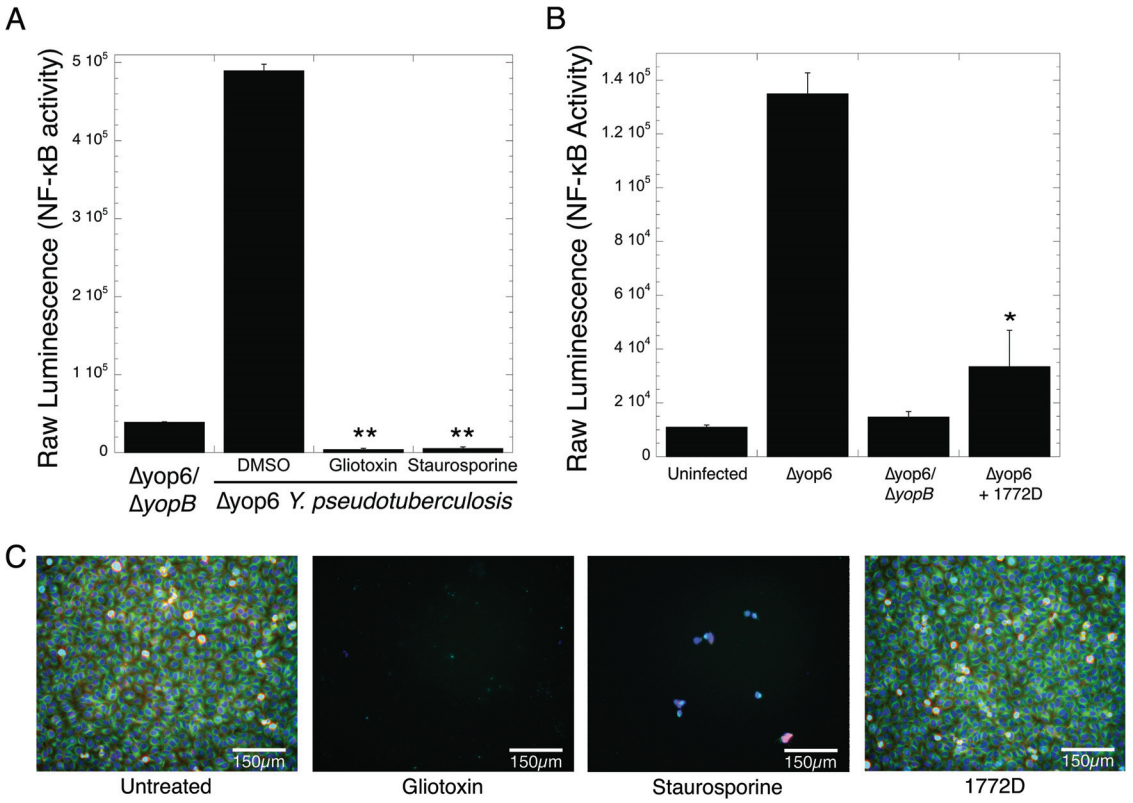

FIG 2 Identification of natural-product fractions that inhibit T3SS-driven NF-κB activation but are not toxic to mammalian cells. (A and B) HEK293T cells expressing an NF-κB-inducible luciferase reporter gene were infected with *Y. pseudotuberculosis* Δ*yop6* Δ*yopB* (nonfunctional T3SS) or Δ*yop6* (functional T3SS) in the presence or absence of the cytotoxins gliotoxin and staurosporine (A) or prefraction 1772D identified in our HTS (B). Bioluminescence was measured as a readout of T3SS function. The averages and standard errors of the mean (SEM) from two independent experiments are shown. *, $P < 0.05$, and **, $P < 0.005$ (Student *t* test) relative to HEK293T cells infected with the Δ*yop6* strain and DMSO treated. (C) HeLa cells were incubated with DMSO, staurosporine, or prefraction 1772D for 19 h. Fixed cells were stained for tubulin (green), actin (red), DNA (blue), and phosphohistone H3 (to indicate mitosis) (cyan).

Of the remaining 138 prefractions, we hypothesized that some may contain compounds with general antibiotic activity, blocking *Y. pseudotuberculosis* replication. In a separate study, Wong et al. carried out antibiotic mode-of-action profiling on the same natural-products library using a panel of bacteria. Based on their findings, we eliminated four additional prefractions that inhibited *Y. pseudotuberculosis* growth in broth culture (15) (see Dataset S1 in the supplemental material).

Finally, we eliminated 48 additional prefractions that caused HeLa cell cytoxicity in the study carried out by Schulze et al. (14) but did not reduce NF-κB activity in HEK293T cells to the very low levels seen with staurosporine or gliotoxin (see Dataset S1 in the supplemental material). This discrepancy in toxicity may be due to the cell types used (HeLa versus HEK293T) or the time frame of the experiments (19 h versus 4 h). However, T3SS inhibitors that are also cytotoxic toward mammalian cells would be significantly less useful as T3SS research probes and pretherapeutics. Therefore, we eliminated prefractions displaying such dual activity, leaving 86 prefractions in our final pool.

Estimating an average of 11 compounds per prefraction, and one compound per bioactive prefraction responsible for T3SS-inhibitory activity, the hit rate per compound is ~0.3%. This hit rate is within the range of previously published T3SS inhibitor screens (16–21).

Identification of piericidins with T3SS-inhibitory activity. We selected 21 prefractions for further investigation by separating the small molecules within each prefraction using liquid chromatography-mass spectrometry (LC-MS) to generate "one compound-one well" peak libraries for secondary screening. This approach provides mass spectrometric, UV absorbance, and retention time data for all active constituents and permits direct identification of bioactive compounds from active fractions. We then used these peak libraries to repeat the experiment described above (Fig. 1) and identified individual constituents able to inhibit T3SS-driven NF-κB activation.

We focused on prefraction 1772D, which caused a 3.5-fold decrease in T3SS-driven NF-κB activation (Fig. 2B). In comparison to staurosporine, prefraction 1772D did not cause gross changes in HeLa cell morphology in the absence of bacteria (Fig. 2C), indicating that the compounds in the prefraction are not grossly cytotoxic to mammalian cells. Upon further separation, prefraction 1772D yielded four fractions, corresponding to 31, 32, 43, and 44 min of retention time on the HPLC, that exhibited significant inhibition of T3SS-driven NF-κB activation (Fig. 3A) and displayed tractable chromatography for compound isolation (Fig. 3B). We regrew *Streptomyces* sp. strain RL09-253-HVS-A, which produced prefraction 1772D, and reisolated and purified the bioactive compounds. The structures of two related compounds found in 1772D fractions 31, 32, 43, and 44 were determined using a combination of NMR and MS experiments (Fig. 3C; see Fig. S2 and S3 in the supplemental material). We identified one compound as the piericidin derivative Mer-A

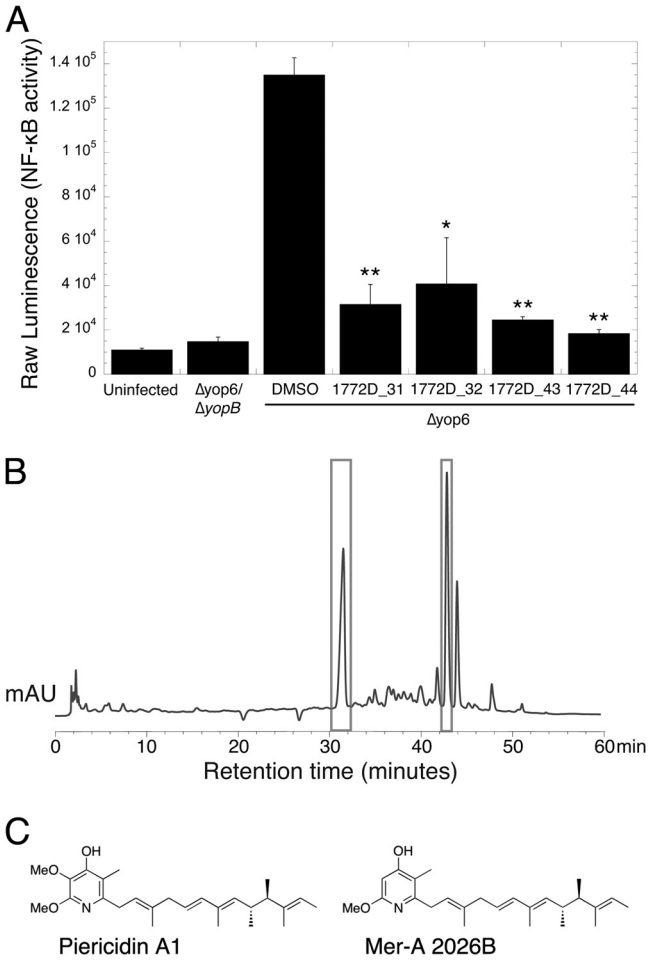

FIG 3 Piericidin A1 and the piericidin derivative Mer-A 2026B are the bioactive constituents of prefraction 1772D. (A) Prefraction 1772D was fractionated by HPLC-MS, and the eluent was rescreened to identify the active constituents. Fractions from minutes 31, 32, 43, and 44 contained compounds that inhibited T3SS-driven NF-κB activation in HEK293T cells. The averages and SEM are shown. *, $P < 0.05$, and **, $P < 0.005$ (Student *t* test) relative to HEK293T cells infected with the Δ*yop6* strain and DMSO treated from two independent experiments. (B) Chromatogram (HPLC trace) of prefraction 1772D. Bioactive 1772D fractions 31, 32, 43, and 44 are boxed and contained compounds with related UV absorbance profiles. mAU, milliabsorbance units. (C) Structures of piericidin A1 and the piericidin derivative Mer-A 2026B identified through standard MS and NMR analyses.

2026B and the other as piericidin A1 (22–24). Piericidins have previously characterized activity as insecticides, vasodilators, and inhibitors of the mitochondrial NADH dehydrogenase and as general antibiotics against certain bacteria (22, 23, 25–27).

Mer-A 2026B and piericidin A1 do not inhibit *Yersinia* growth. To confirm that the piericidins did not affect bacterial replication, we performed growth curves of *Y. pseudotuberculosis* in the presence of the purified compounds at 26°C and 37°C and monitored bacterial growth by optical density (Fig. 4). Piericidin-treated *Y. pseudotuberculosis* grew as well as or better than DMSO-treated bacteria at all tested concentrations up to 143 μM, in contrast to the known antibiotic kanamycin. We also performed more sensitive 24-h growth curves by serially diluting and plating cultures after 0, 3, 6, and 24 h of growth (see Fig. S4 in the supplemental material). We observed no difference in bacterial replication between DMSO- and 143 μM piericidin-treated *Y. pseudotuberculosis* at all time points. As expected, we could not recover any CFU from kanamycin-treated cultures at 3, 6, or 24 h of growth.

Mer-A 2026B and piericidin A1 inhibit secretion of Yop proteins *in vitro*. We evaluated the ability of *Y. pseudotuberculosis* to secrete effector Yop proteins into broth culture in the presence of the piericidins or five previously identified, commercially available T3SS inhibitors (see Fig. S5 in the supplemental material). MBX-1641 and aurodox were shown to reduce *in vitro* type III secretion by *Yersinia pestis* and *Escherichia coli*, respectively, and were chosen as positive controls. In contrast, C15, C22, and C24 were shown to inhibit translocation of effector proteins inside host cells, but not Yop secretion *in vitro*, and were chosen as negative controls (16). We grew *Y. pseudotuberculosis* in the presence of purified compounds or DMSO for 2 h at 37°C in the absence of calcium (T3SS-inducing conditions). We then precipitated the secreted proteins from the supernatant and analyzed relative protein abundance using SDS-PAGE analysis.

Mer-A 2026B at a concentration of 71 μM reduced secretion of the T3SS effector YopE by 45% ($P < 0.02$), while lower concentrations of inhibitor demonstrated a dose-dependent decrease in inhibition (Fig. 5). Piericidin A1 blocked type III secretion by 65% (Fig. 5B). MBX 1641 (17) and C15 (16) at a concentration of 71 μM also significantly reduced YopE secretion, although this inhibition was only 22 to 33% ($P < 0.05$ and $P < 0.04$, respectively). In our hands, C22 and C24 did not significantly reduce T3S, which was consistent with the original report (16). However, C15 did block *in vitro* secretion. Aurodox (21) did not significantly inhibit YopE secretion at the highest concentration used, 12.5 μM (Fig. 5B). We chose not to test aurodox at 71 μM, as Kimura et al. found concentrations above 12.5 μM cytotoxic to *E. coli*.

Mer-A 2026B and piericidin A1 inhibit translocation of YopM. To analyze the ability of the piericidins to block translocation of *Y. pseudotuberculosis* T3SS effector proteins, we measured the translocation of a plasmid-encoded YopM-Bla reporter protein inside CHO cells using the fluorescent β-lactamase substrate CCF2-AM (28). In this assay, the CHO cells are loaded with the CCF2-AM dye, which normally fluoresces green. If the YopM–β-lactamase chimeric fusion is translocated into these cells, the dye is cleaved and the cells fluoresce blue, providing a quantifiable readout of T3SS-mediated translocation.

The piericidin derivative Mer-A 2026B significantly reduced YopM translocation into CHO cells at all concentrations (Fig. 6), ranging from 9 μM to 143 μM. The 71 μM concentration displayed the most robust T3SS inhibition, 75% ($P < 0.005$). Piericidin A1 also significantly diminished YopM–β-lactamase translocation at concentrations of 36 μM and greater (Fig. 6C). These results validate the notion that the piericidins identified through our screen inhibit T3SS effector translocation into eukaryotic cells.

DISCUSSION

In this study, we screened 2,560 marine-derived extracts from our in-house natural-products library and identified two previously undiscovered T3SS inhibitors: piericidin A1 and the piericidin derivative Mer-A 2026B. These compounds blocked the *Y. pseudotuberculosis* T3SS in three distinct assays without cytotoxic effects on *Yersinia* or mammalian cells.

T3SS inhibitors belong to a novel antibiotic class called virulence blockers, which are designed to prevent normal infection by

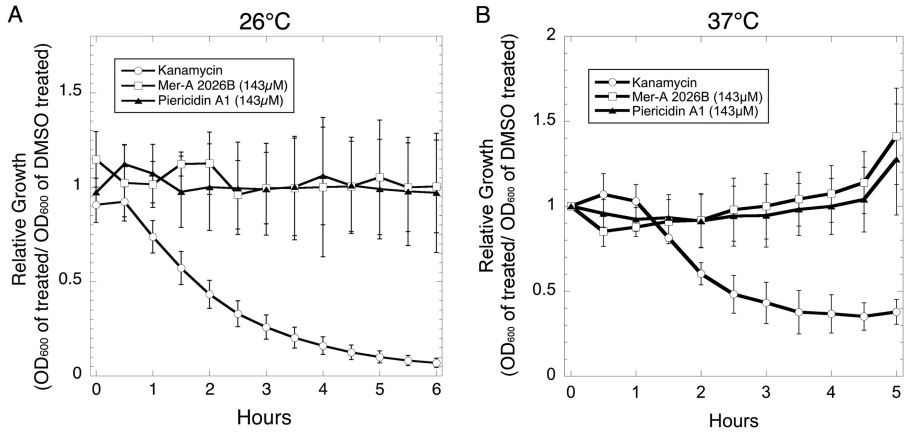

FIG 4 Piericidin A1 and Mer-A 2026B do not affect *Y. pseudotuberculosis in vitro* growth. Wild-type *Y. pseudotuberculosis* was grown at 23°C or 37°C with continuous shaking in the presence of DMSO, kanamycin, or piericidins. The averages ± SEM of values from three independent experiments [calculated as follows: (OD_{600} compound treated)/(OD_{600} DMSO treated)] are shown.

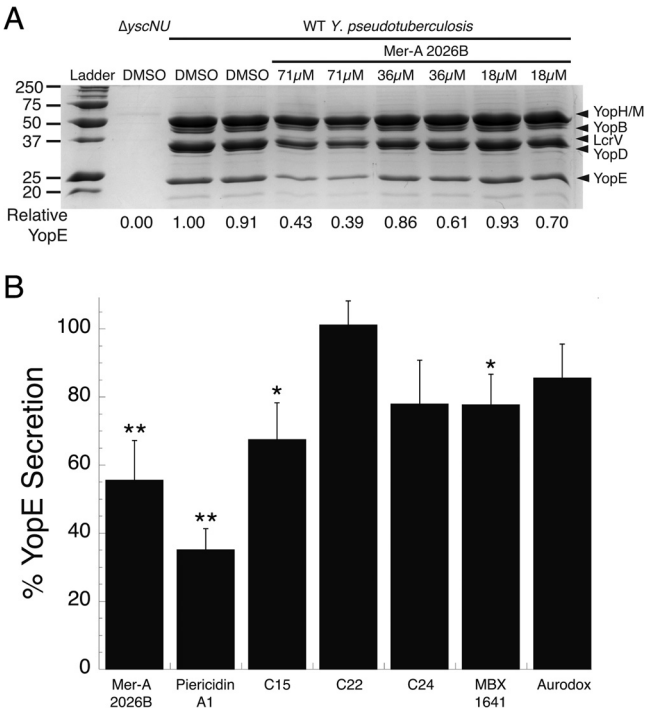

FIG 5 Mer-A 2026B and piericidin A1 inhibit *Yersinia* type III secretion *in vitro* more robustly than several previously identified T3SS inhibitors. (A) WT *Y. pseudotuberculosis* was incubated for 2 h under type III secretion-inducing conditions in the presence of various concentrations of the piericidin derivative Mer-A 2026B or DMSO. The secretome was precipitated with trichloroacetic acid and analyzed by SDS-PAGE analysis. The intensity of the Coomassie blue-stained band consistent with the size of YopE was quantified relative to DMSO-treated *Y. pseudotuberculosis*. The identity of the indicated YopE band was confirmed by Western blotting (data not shown). (B) The experiment in panel A was repeated using piericidin A1 and the previously identified, commercially available T3SS inhibitors C15, C22, and C24 (16) and MBX1641 (17) at a final concentration of 71 μM (data not shown) (16, 17, 21). Aurodox was used at a final concentration of 12.5 μM (21). The average inhibition of YopE secretion by the T3SS inhibitors compared to DMSO [(inhibitor-treated YopE band intensity)/(DMSO-treated YopE band intensity)] and SEM from 3 or 4 independent experiments is shown. *, $P < 0.05$, and ** $P < 0.02$ (Student *t* test) relative to DMSO-treated WT *Y. pseudotuberculosis*.

disarming pathogenic bacteria. This is in contrast to traditional antibiotics, which kill both pathogens and commensals alike by targeting essential pathways, such as cell wall synthesis or translation (11, 12). Proposed bacterial targets for virulence blockers include quorum-sensing mechanisms, toxin expression, pili, and secretion systems (10). Many of these virulence factors, including T3SS (1), are rarely expressed in nonpathogenic bacteria, so the majority of the microbiota should be unaffected by virulence-targeted treatment. This narrower selective pressure may slow evolution of resistance to T3SS inhibitors (29). In support of this, recent evidence suggests that resistance to traditional antibiotics often arises in the abundant commensal flora and is then horizontally transferred to the scarcer pathogens (12, 30).

The HTS reported here is the first T3SS inhibitor screen that uses the host immune response to measure T3SS function (6). *Y. pseudotuberculosis* induces NF-κB activation in HEK293T cells dependent on expression of a functional T3SS (13). While the mechanism behind this NF-κB activation remains unclear, several bacterial genetic requirements have been resolved. A *Y. pseudotuberculosis* Δ*yopB* mutant expresses T3SS injectisomes on its surface but cannot make YopB-dependent pores on host cell membranes and therefore cannot facilitate the translocation of T3SS cargo inside target host cells. Importantly, a Δ*yopB* mutant does not trigger NF-κB activation (13). Therefore, NF-κB activation in HEK293T cells can be used as an indicator of whether the *Y. pseudotuberculosis* T3SS is functional. We reasoned that small molecules that inhibit T3SS assembly or YopB secretion would block NF-κB activation during *Y. pseudotuberculosis* infection of HEK293T cells. Using NF-κB activation as a readout of T3SS function in an HTS, we found two related compounds that (i) inhibit secretion of Yop proteins *in vitro*, which requires assembly of the T3SS apparatus (31), and (ii) block translocation of YopM inside mammalian cells, which requires YopB-dependent pore formation (32). Using these orthogonal assays, we validated that our HTS can identify genuine T3SS inhibitors.

A benefit of our HTS design is the recognition and exclusion of small molecules that are cytotoxic to mammalian cells. We observed that compounds toxic to mammalian cells, such as staurosporine and gliotoxin, inhibit NF-κB activation in our HTS to a level below that induced by a Δ*yopB* mutant in the absence of

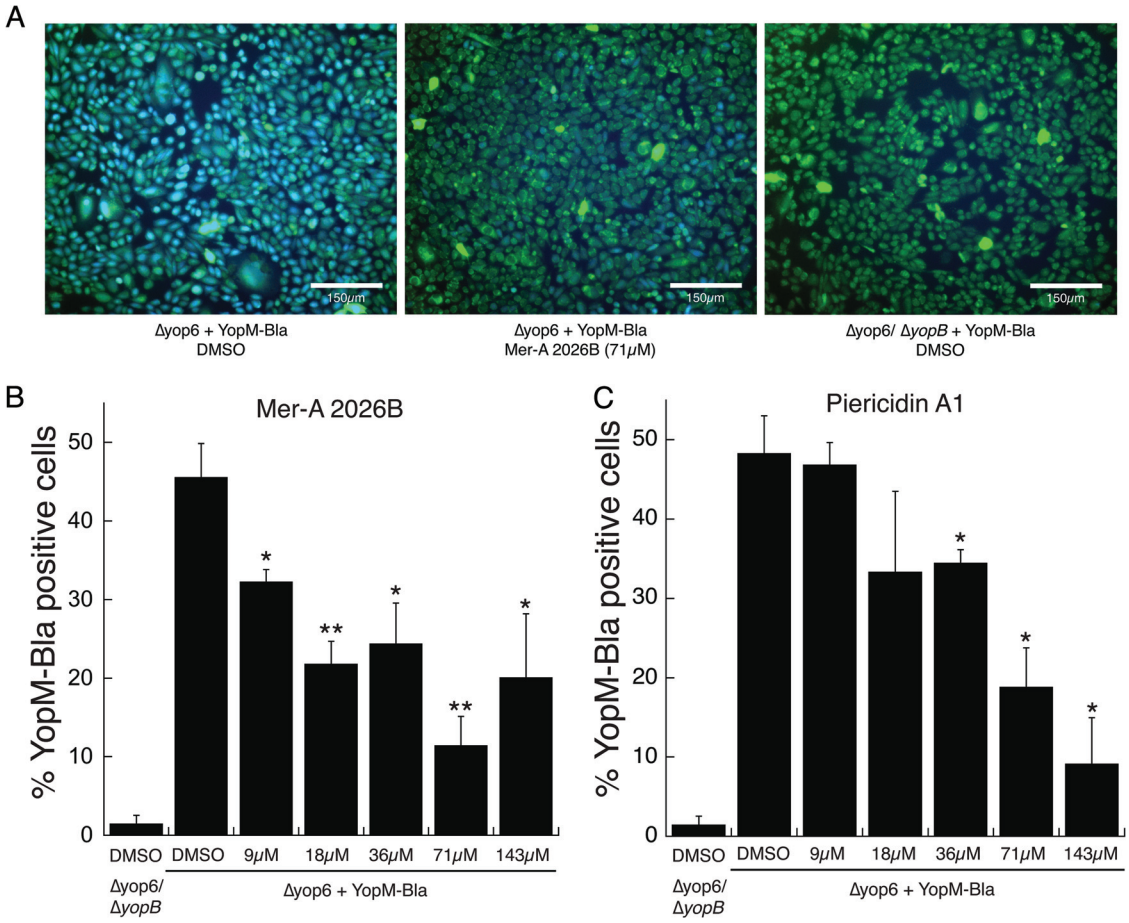

FIG 6 Piericidin A1 and Mer-A 2026B prevent translocation of YopM-Bla into eukaryotic cells. CCF2-loaded CHO cells were infected with *Y. pseudotuberculosis* expressing a YopM-Bla reporter. The relative efficacy of YopM translocation was measured by quantifying the intensities of uncleaved CCF2 (green) and cleaved CCF2 (blue). Shown are representative images (A) and the average percentage of blue cells (those that were injected with YopM-Bla) out of the total green cells (those that took up CCF2) and SEM from 3 or 4 independent experiments (B). *, $P < 0.05$, and **, $P < 0.005$ (Student *t* test) relative to DMSO-treated *Y. pseudotuberculosis*.

inhibitors (Fig. 2A). This enabled us to differentiate generally cytotoxic compounds from those with putative T3SS-inhibitory activity. In fact, 92% of natural-product-containing fractions that inhibited NF-κB activation to a level below that induced by Δ*yopB* also caused HeLa cytotoxicity, as measured in a separate study using the same natural-products library (14). This aspect of our HTS may be particularly useful for screening potent compound libraries not yet tested against mammalian cells.

Only one other published HTS for T3SS inhibitors has made use of nucleated cells, where the authors used a Yop–β-lactamase translocation assay similar to the one used in Fig. 6 to validate our HTS results (16). Two other studies by Iwatsuki et al. and Kimura et al. published HTSs analyzing host-pathogen interactions with anucleate cells, measuring T3SS-mediated red blood cell lysis (21, 33). One major advantage of the HTS presented here is the use of a relatively low MOI of 7. We found that using a low MOI enabled greater sensitivity for identification of bioactive compounds (data not shown).

Piericidins were first reported in the 1960s as insecticides and inhibitors of mitochondrial electron transport (25). Later, the piericidin derivative Mer-A 2026B was discovered and proposed to have vasodilator activity (22, 23). However, we observed no cell death or morphological changes to HeLa cells incubated with ≤250 μM piericidins for 19 h (Fig. 2C) (reference 14 and unpublished data). It is possible that piericidin A1 and/or Mer-A 2026B impact only the physiology of specific eukaryotic cell types or that the cytological profiling study performed on HeLa cells incubated with these compounds was not sensitive enough to detect changes to mitochondrial electron transport. In addition, despite reports in the literature identifying piericidins as antibiotics (26), we observed no effect of either piericidin A1 or Mer-A 2026B on *Y. pseudotuberculosis* growth in broth culture (Fig. 4; see Fig. S5 in the supplemental material). A separate study tested the 1772D prefraction containing piericidin A1 and Mer-A 2026B against a panel of 15 bacterial pathogens and found inhibitory activity against only two Gram-positive bacteria, *Bacillus subtilis* and *Listeria ivanovii* (15; W. R. Wong and R. G. Linington, unpublished data). This indicates that piericidin A1 and Mer-A 2026B do not broadly affect bacterial growth and have a specific impact on the T3SS in *Yersinia*.

Interestingly, piericidins and the previously discovered T3SS inhibitor aurodox both have pyridine rings (Fig. 3C; see Fig. S4 in the supplemental material) (21). This moiety is relatively rare in nature, and it is tempting to speculate that these compounds may

share a molecular target. While aurodox was effective against the *E. coli* and *Citrobacter rodentium* T3SSs (21), in our study aurodox did not significantly inhibit Yop secretion by *Y. pseudotuberculosis* (Fig. 5B). It is possible that if aurodox and the piericidins target the same molecular structure, aurodox is more active against T3SS belonging to the SPI-2 family, such as that carried by *E. coli* and *Citrobacter*, while the piericidins are more active against Ysc family T3SS, such as that utilized by all three pathogenic *Yersinia* species (1). Like the piericidins, aurodox has antibiotic activity toward Gram-positive bacteria but is thought to stall ribosomes by binding to the active domain of elongation factor Tu (34). More work is needed to identify the molecular targets of the piericidins and aurodox in Gram-positive and T3SS-expressing Gram-negative bacteria.

In addition to aurodox, we compared the relative abilities of the piericidins and several previously identified T3SS inhibitors to block Yop secretion *in vitro*. Mer-A 2026B and piericidin A1 demonstrated the most robust T3SS inhibition, reducing YopE secretion into the culture medium by 45% and 65%, respectively. The fact that we did not observe a complete block of type III secretion may suggest an indirect mechanism of inhibition. MBX 1641, originally identified as an inhibitor of the *Pseudomonas aeruginosa* T3SS by Aiello et al. (17), showed a modest but significant reduction in effector secretion. In contrast, only one of three compounds discovered by Harmon et al. inhibited type III secretion in our *in vitro* assay. We were surprised to observe this inhibition by C15, as the exhaustive study by Harmon et al. proposed that their compounds interfered with pore formation or host cell contact (16). One possible reason for the discrepancy is the higher concentration of compound used in our assay (71 μM versus 60 μM).

An obvious challenge for the field of virulence blockers is a lack of standardized drug activity assays. Traditional antibiotics stall growth or kill bacteria, and therefore, one can compare drug efficacy by assaying for the MIC for growth. *In vitro* measurements of secreted effectors may be one useful tool for comparing efficacy among secretion system inhibitors. Other classes of virulence blockers require their own comparative assays, and appropriate dosing will need to be established early in animal studies.

As T3SS are highly conserved among Gram-negative pathogens, one inhibitor could be broadly effective against a number of infections. In fact, the best-characterized T3SS inhibitors, salicylidene acylhydrazides, have been successful against six genera of bacteria (6). Conversely, narrow-spectrum drugs are likely to be more useful in the near future as point-of-care nucleic acid testing enters the clinic and allows rapid, accurate identification of infectious agents (35, 36). Since T3SS inhibitors are less likely to generate resistance, they also have potential as prophylactics for humans or in livestock. Follow-up studies on piericidins will determine if these compounds can block type III secretion by other pathogens and focus on identifying the molecular target(s). As flagella are evolutionarily related to T3SS, it will be important to determine whether piericidins affect flagellar motility. Lastly, structure-activity relationship studies could increase the potency of piericidins while abrogating potential off-target effects.

In summary, we have discovered two small molecules, piericidin A1 and Mer-A 2026B, with anti-T3SS activity. These compounds blocked *in vitro* secretion and translocation of T3SS effectors inside host cells but were not toxic to mammalian cells or *Yersinia*. Furthermore, the piericidins were more robust in blocking Yop secretion than several recently discovered T3SS inhibitors, justifying further study of this new class of T3SS inhibitor.

ACKNOWLEDGMENTS

We thank Halie Miller for critical reading of the manuscript. We thank Melanie Marketon for the YopM–β-lactamase reporter plasmid. We thank Scott Lokey for access to the UCSC Chemical Screening Center.

This work was supported by the California Institute for Quantitative Biosciences (V.A., M.C.D., and W.R.W.) and The Malaysian Biotechnology Corporation (W.R.W.).

REFERENCES

1. **Cornelis GR.** 2006. The type III secretion injectisome. Nat. Rev. Microbiol. **4:**811–825. http://dx.doi.org/10.1038/nrmicro1526.
2. **Morris JG, Potter ME.** 2013. Foodborne infections and intoxications, 4th ed. Academic Press, Waltham, MA.
3. **Projan SJ, Bradford PA.** 2007. Late stage antibacterial drugs in the clinical pipeline. Curr. Opin. Microbiol. **10:**441–446. http://dx.doi.org/10.1016/j.mib.2007.08.007.
4. **Boucher HW, Talbot GH, Benjamin DK, Jr, Bradley J, Guidos RJ, Jones RN, Murray BE, Bonomo RA, Gilbert D.** 2013. 10 x '20 progress—development of new drugs active against gram-negative bacilli: an update from the Infectious Diseases Society of America. Clin. Infect. Dis. **56:**1685–1694. http://dx.doi.org/10.1093/cid/cit152.
5. **Moraes TF, Spreter T, Strynadka NC.** 2008. Piecing together the type III injectisome of bacterial pathogens. Curr. Opin. Struct. Biol. **18:**258–266. http://dx.doi.org/10.1016/j.sbi.2007.12.011.
6. **Duncan MC, Linington RG, Auerbuch V.** 2012. Chemical inhibitors of the type three secretion system: disarming bacterial pathogens. Antimicrob. Agents Chemother. **56:**5433–5441. http://dx.doi.org/10.1128/AAC.00975-12.
7. **Bleves S, Cornelis GR.** 2000. How to survive in the host: the *Yersinia* lesson. Microbes Infect. **2:**1451–1460. http://dx.doi.org/10.1016/S1286-4579(00)01300-9.
8. **Bliska JB, Wang X, Viboud GI, Brodsky IE.** 2013. Modulation of innate immune responses by *Yersinia* type III secretion system translocators and effectors. Cell. Microbiol. **15:**1622–1631. http://dx.doi.org/10.1111/cmi.12164.
9. **Matsumoto H, Young GM.** 2009. Translocated effectors of *Yersinia*. Curr. Opin. Microbiol. **12:**94–100. http://dx.doi.org/10.1016/j.mib.2008.12.005.
10. **Clatworthy AE, Pierson E, Hung DT.** 2007. Targeting virulence: a new paradigm for antimicrobial therapy. Nat. Chem. Biol. **3:**541–548. http://dx.doi.org/10.1038/nchembio.2007.24.
11. **Baron C.** 2010. Antivirulence drugs to target bacterial secretion systems. Curr. Opin. Microbiol. **13:**100–105. http://dx.doi.org/10.1016/j.mib.2009.12.003.
12. **Keyser P, Elofsson M, Rosell S, Wolf-Watz H.** 2008. Virulence blockers as alternatives to antibiotics: type III secretion inhibitors against Gram-negative bacteria. J. Intern. Med. **264:**17–29. http://dx.doi.org/10.1111/j.1365-2796.2008.01941.x.
13. **Auerbuch V, Golenbock DT, Isberg RR.** 2009. Innate immune recognition of *Yersinia pseudotuberculosis* type III secretion. PLoS Pathog. **5:**e1000686. http://dx.doi.org/10.1371/journal.ppat.1000686.
14. **Schulze CJ, Bray WM, Woerhmann MH, Stuart J, Lokey RS, Linington RG.** 2013. "Function-first" lead discovery: mode of action profiling of natural product libraries using image-based screening. Chem. Biol. **20:**285–295. http://dx.doi.org/10.1016/j.chembiol.2012.12.007.
15. **Wong WR, Oliver AG, Linington RG.** 2012. Development of antibiotic activity profile screening for the classification and discovery of natural product antibiotics. Chem. Biol. **19:**1483–1495. http://dx.doi.org/10.1016/j.chembiol.2012.09.014.
16. **Harmon DE, Davis AJ, Castillo C, Mecsas J.** 2010. Identification and characterization of small-molecule inhibitors of Yop translocation in *Yersinia pseudotuberculosis*. Antimicrob. Agents Chemother. **54:**3241–3254. http://dx.doi.org/10.1128/AAC.00364-10.
17. **Aiello D, Williams JD, Majgier-Baranowska H, Patel I, Peet NP, Huang J, Lory S, Bowlin TL, Moir DT.** 2010. Discovery and characterization of inhibitors of *Pseudomonas aeruginosa* type III secretion. Antimicrob. Agents Chemother. **54:**1988–1999. http://dx.doi.org/10.1128/AAC.01598-09.
18. **Kauppi AM, Nordfelth R, Hagglund U, Wolf-Watz H, Elofsson M.**

2003. Salicylanilides are potent inhibitors of type III secretion in *Yersinia*. Adv. Exp. Med. Biol. **529:**97–100. http://dx.doi.org/10.1007/0-306-48416-1_17.
19. **Pan NJ, Brady MJ, Leong JM, Goguen JD.** 2009. Targeting type III secretion in *Yersinia pestis*. Antimicrob. Agents Chemother. **53:**385–392. http://dx.doi.org/10.1128/AAC.00670-08.
20. **Felise HB, Nguyen HV, Pfuetzner RA, Barry KC, Jackson SR, Blanc MP, Bronstein PA, Kline T, Miller SI.** 2008. An inhibitor of gram-negative bacterial virulence protein secretion. Cell Host Microbe **4:**325–336. http://dx.doi.org/10.1016/j.chom.2008.08.001.
21. **Kimura K, Iwatsuki M, Nagai T, Matsumoto A, Takahashi Y, Shiomi K, Omura S, Abe A.** 2011. A small-molecule inhibitor of the bacterial type III secretion system protects against in vivo infection with *Citrobacter rodentium*. J. Antibiot. **64:**197–203. http://dx.doi.org/10.1038/ja.2010.155.
22. **Kominato K, Watanabe Y, Hirano S, Kioka T, Terasawa T, Yoshioka T, Okamura K, Tone H.** 1995. Mer-A2026A and B, novel piericidins with vasodilating effect. I. Producing organism, fermentation, isolation and biological properties. J. Antibiot. **48:**99–102.
23. **Kominato K, Watanabe Y, Hirano S, Kioka T, Terasawa T, Yoshioka T, Okamura K, Tone H.** 1995. Mer-A2026A and B, novel piericidins with vasodilating effect. II. Physico-chemical properties and chemical structures. J. Antibiot. **48:**103–105.
24. **Schnermann MJ, Boger DL.** 2005. Total synthesis of piericidin A1 and B1. J. Am. Chem. Soc. **127:**15704–15705. http://dx.doi.org/10.1021/ja055041f.
25. **Hall C, Wu M, Crane FL, Takahashi H, Tamura S, Folkers K.** 1966. Piericidin A: a new inhibitor of mitochondrial electron transport. Biochem. Biophys. Res. Commun. **25:**373–377. http://dx.doi.org/10.1016/0006-291X(66)90214-2.
26. **Kimura K, Nakayama S, Nakajima N, Yoshihama M, Miyata N, Kawanishi G.** 1990. A new piericidin rhamnoside, 3′-rhamnopiericidin A1. J. Antibiot. **43:**1341–1343. http://dx.doi.org/10.7164/antibiotics.43.1341.
27. **Matsumoto M, Mogi K, Nagaoka K, Ishizeki S, Kawahara R, Nakashima T.** 1987. New piericidin glucosides, glucopiericidins A and B. J. Antibiot. **40:**149–156. http://dx.doi.org/10.7164/antibiotics.40.149.
28. **Dewoody R, Merritt PM, Houppert AS, Marketon MM.** 2011. YopK regulates the *Yersinia pestis* type III secretion system from within host cells. Mol. Microbiol. **79:**1445–1461. http://dx.doi.org/10.1111/j.1365-2958.2011.07534.x.
29. **Lewis K.** 2013. Platforms for antibiotic discovery. Nat. Rev. Drug Discov. **12:**371–387. http://dx.doi.org/10.1038/nrd3975.
30. **Schjorring S, Krogfelt KA.** 2011. Assessment of bacterial antibiotic resistance transfer in the gut. Int. J. Microbiol. **2011:**312956. http://dx.doi.org/10.1155/2011/312956.
31. **Deane JE, Abrusci P, Johnson S, Lea SM.** 2010. Timing is everything: the regulation of type III secretion. Cell. Mol. Life Sci. **67:**1065–1075. http://dx.doi.org/10.1007/s00018-009-0230-0.
32. **Neyt C, Cornelis GR.** 1999. Insertion of a Yop translocation pore into the macrophage plasma membrane by *Yersinia enterocolitica*: requirement for translocators YopB and YopD, but not LcrG. Mol. Microbiol. **33:**971–981. http://dx.doi.org/10.1046/j.1365-2958.1999.01537.x.
33. **Iwatsuki M, Uchida R, Yoshijima H, Ui H, Shiomi K, Matsumoto A, Takahashi Y, Abe A, Tomoda H, Omura S.** 2008. Guadinomines, type III secretion system inhibitors, produced by *Streptomyces* sp. K01-0509. I: taxonomy, fermentation, isolation and biological properties. J. Antibiot. **61:**222–229. http://dx.doi.org/10.1038/ja.2008.32.
34. **Parmeggiani A, Swart GW.** 1985. Mechanism of action of kirromycin-like antibiotics. Annu. Rev. Microbiol. **39:**557–577. http://dx.doi.org/10.1146/annurev.mi.39.100185.003013.
35. **Bissonnette L, Bergeron MG.** 2010. Diagnosing infections: current and anticipated technologies for point-of-care diagnostics and home-based testing. Clin. Microbiol. Infect. **16:**1044–1053. http://dx.doi.org/10.1111/j.1469-0691.2010.03282.x.
36. **Niemz A, Ferguson TM, Boyle DS.** 2011. Point-of-care nucleic acid testing for infectious diseases. Trends Biotechnol. **29:**240–250. http://dx.doi.org/10.1016/j.tibtech.2011.01.007.
37. **Bliska JB, Guan KL, Dixon JE, Falkow S.** 1991. Tyrosine phosphate hydrolysis of host proteins by an essential *Yersinia* virulence determinant. Proc. Natl. Acad. Sci. U. S. A. **88:**1187–1191. http://dx.doi.org/10.1073/pnas.88.4.1187.
38. **Balada-Llasat JM, Mecsas J.** 2006. *Yersinia* has a tropism for B and T cell zones of lymph nodes that is independent of the type III secretion system. PLoS Pathog. **2:**e86. http://dx.doi.org/10.1371/journal.ppat.0020086.